Inertia-gravity waves in the mesosphere observed by the PANSY radar

Ryosuke Shibuya[*1], Kaoru Sato[1] and Masaki Tsutsumi[2]

[1]The University of Tokyo, Japan

[2]National Institute of Polar Research, Japan

1. Introduction

Geller et al. (2013)

Absolute GW momentum flux

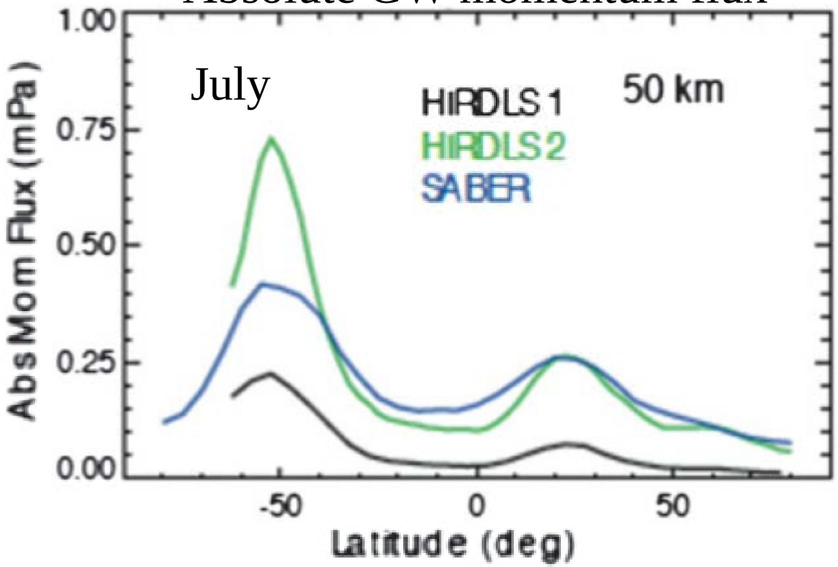

U & $\rho u'w'$ Sato et al. (2009) July

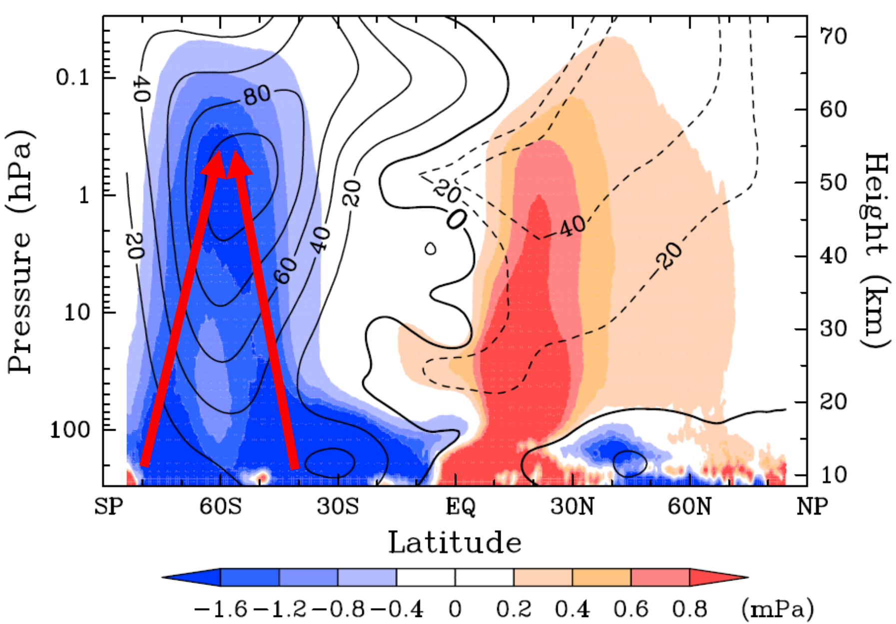

- The largest flux occurs in Southern winter Hemisphere at the south of 50ºS (Geller et al., 2013)
  - — Such a peak was simulated in a vertically high-resolution AGCM (KANTO, watanabe et al., 2008)
  - — $\rho_0\overline{u'w'}$ exhibits a slanted structure, indicating the existence of dominant paths of GW propagation (Sato et al., 2009)
- GWs around 60ºS have an significant impact on a cold-bias problem in CCMs (McLandress et al., 2012)

Observational studies of GWs in the polar region are quite important
(e.g., Hertzog et al., 2008;
VORCORE superpressure balloon)

1. Introduction

■ The PANSY radar (Sato et al., 2014)

— installed at Syowa Station (39°E, 69°S)

— the first MST/IS radar in the Antarctic (since 30 April 2012)

- Vertical profiles of three-dimensional wind vectors can be estimated with Δt=2.5min, Δz=150m (z = 1.5-22 km) and Δz=600m (z = 60-80 km)
- The accuracy of line-of-sight velocity is 0.1 m s^{-1}

- The first successful observation with a complete system was performed in 17-24 March 2015
- In this period, a large solar flare event occurred (Kataoka et al., 2015)

— strong wave-like wind disturbances with a period of about 12 h were observed in the mesosphere

Purpose of this study

To elucidate the dynamical characteristics of quasi 12-h disturbances using the high-resolution observation and a numerical model

2. Observational results

Eastward line-of-sight velocities

$V_{+\vartheta} = u \sin\vartheta + w \cos\vartheta \;\; (\vartheta = 10°)$

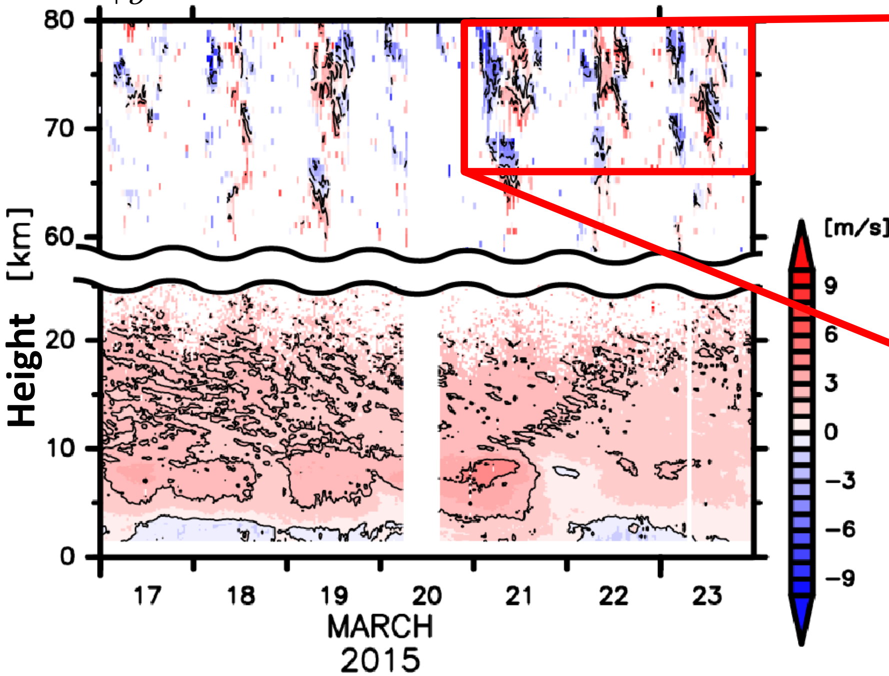

$u \sin\theta + w \cos\theta$

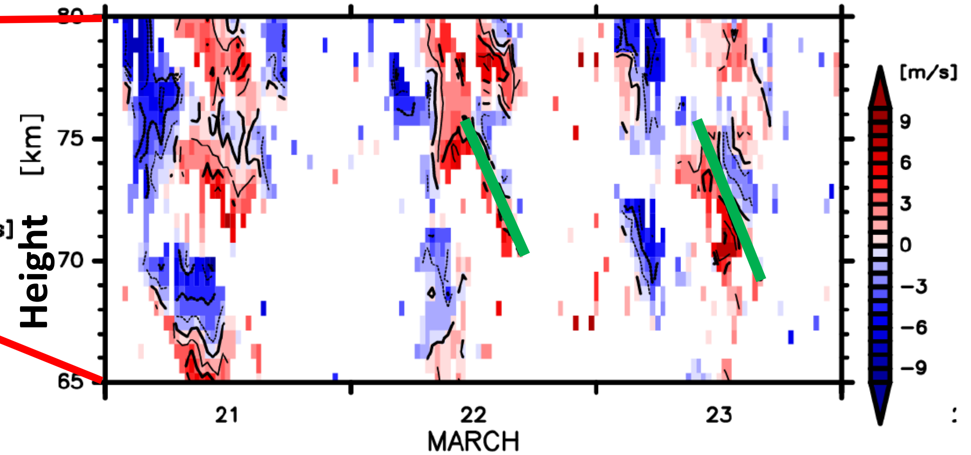

$u \sin\theta - w \cos\theta$

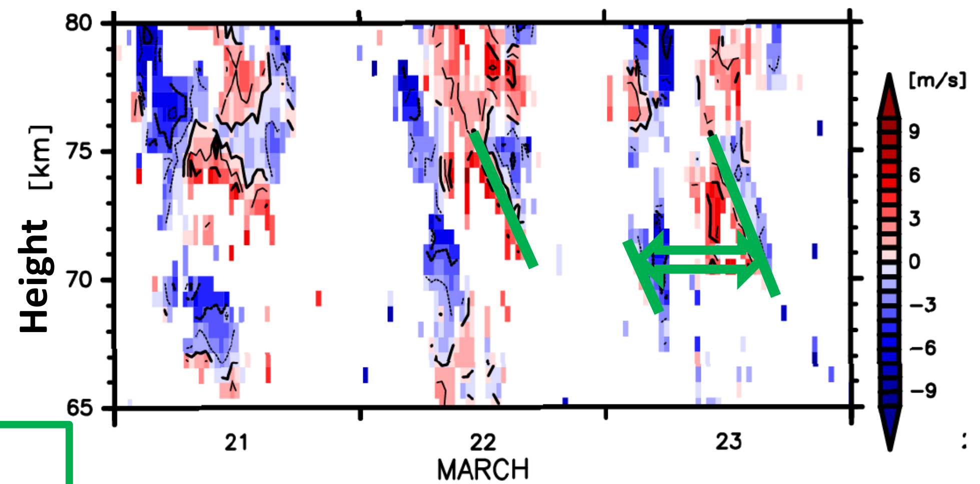

- Clear disturbances propagating phases downward are observed in the mesosphere
- The phase velocity and the wave period are estimated:

$C_{pz} = -0.3 \text{ m s}^{-1}$

$\tau = 2\pi/\omega =$ **12.3 h** $\Rightarrow \lambda_z = 13.7 \text{ km}$

3. Numerical setup for a non-hydrostatic model simulation

・In order to examine spatial structures of the disturbances, a non-hydrostatic numerical simulation was performed

■ NICAM (Satoh et al., 2008) : Nonhydrostatic ICosahedral Atmospheric Model

— No cumulous and GW parameterizations

- Time integration:
  00 UTC 17 – 00 UTC 24 March 2015
- Initial condition:
  MERRA reanalysis data
- Horizontal grid structure:
  stretched and nearly-uniform grid system ($\triangle x \sim 35$ km) to the south of 30°S centered at the south pole (glevel =7)
- Vertical grid structure:
  L217 ($\triangle z = 400$ m) with the model top of z = 87 km

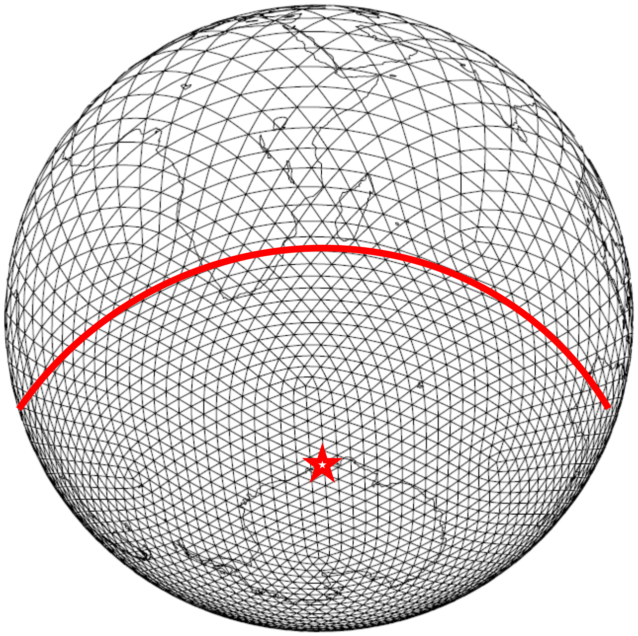

Shibuya et al. (accepted)

4. Numerical results: Comparison with the observation

$$u \sin \vartheta + w \cos \vartheta$$

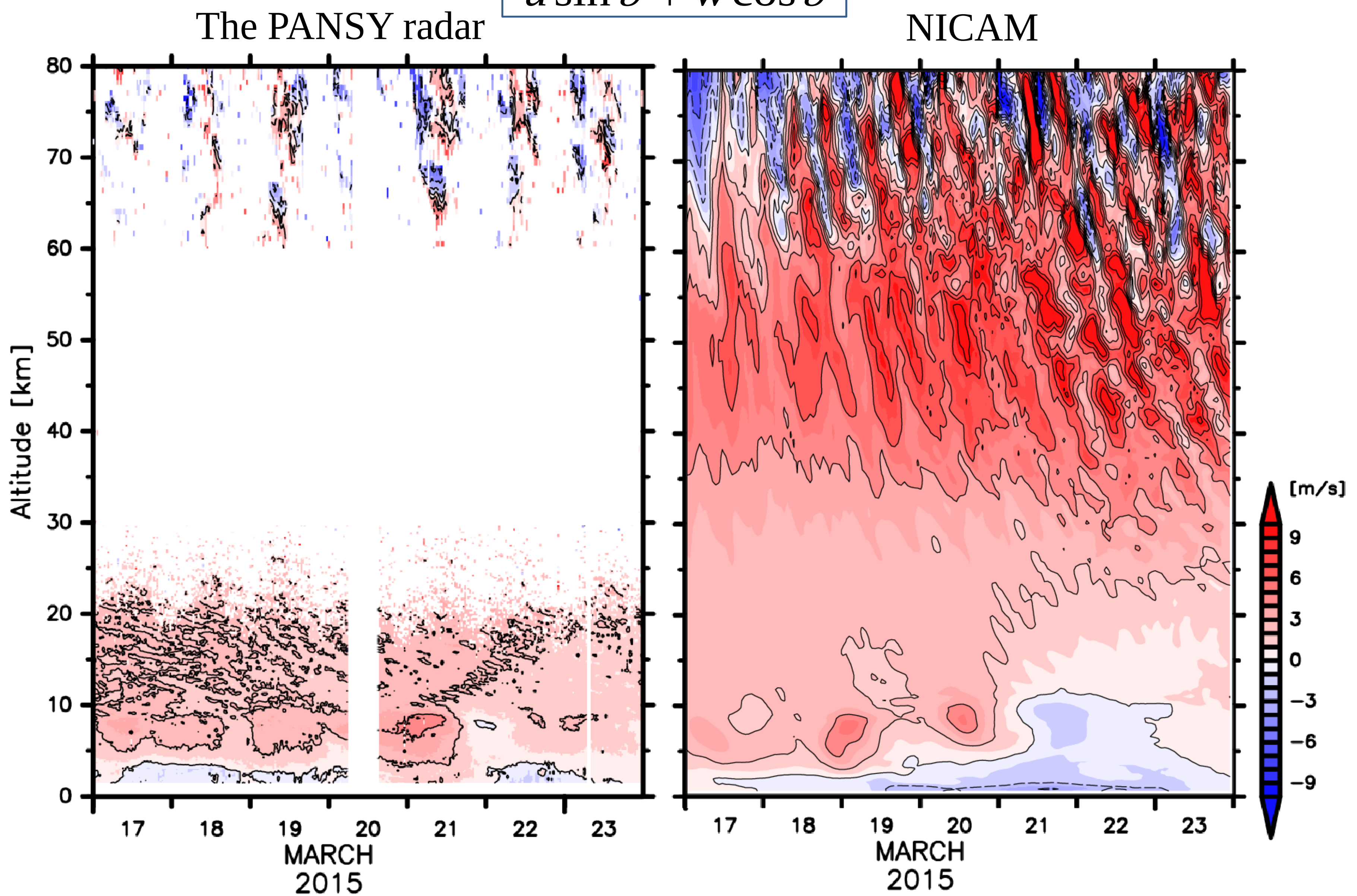

・We have separated wave components to several types of waves:

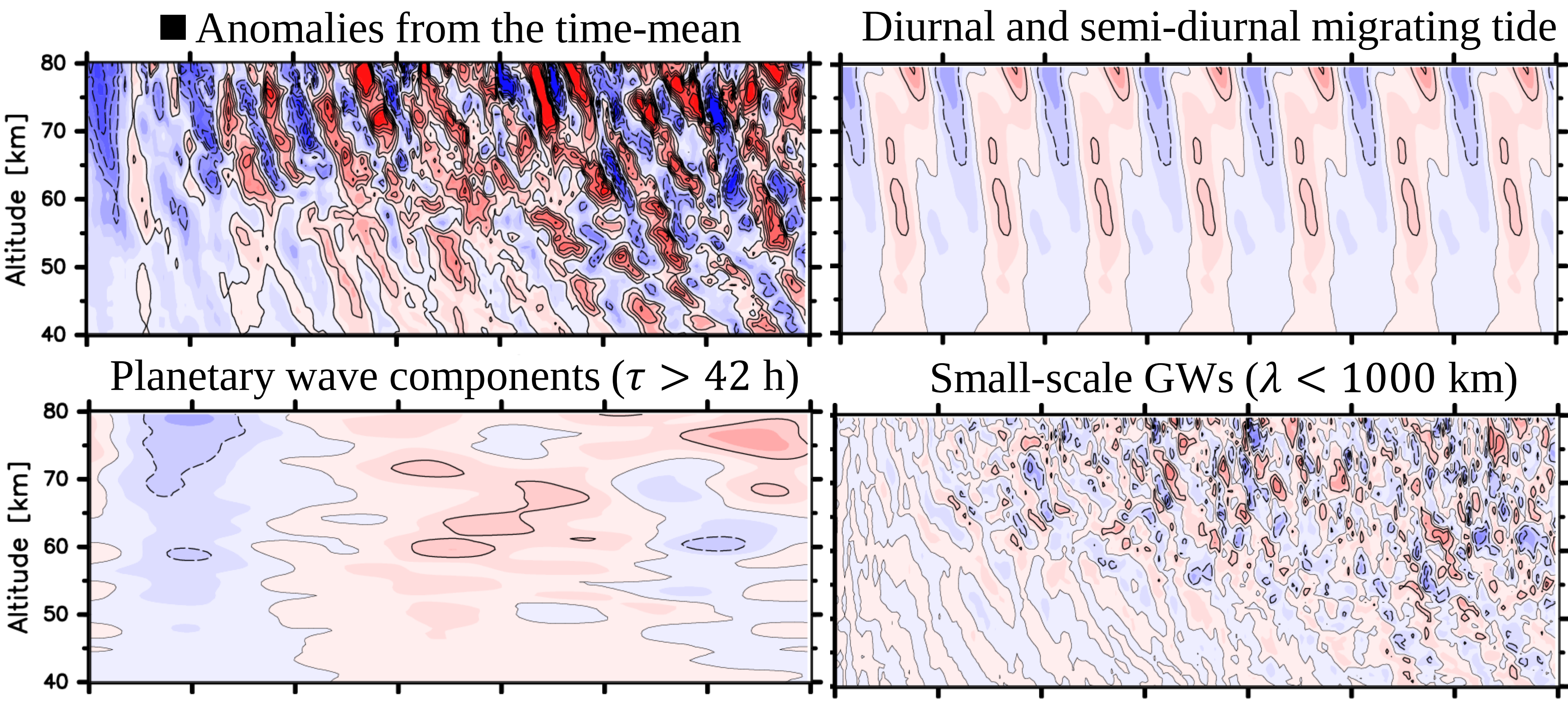

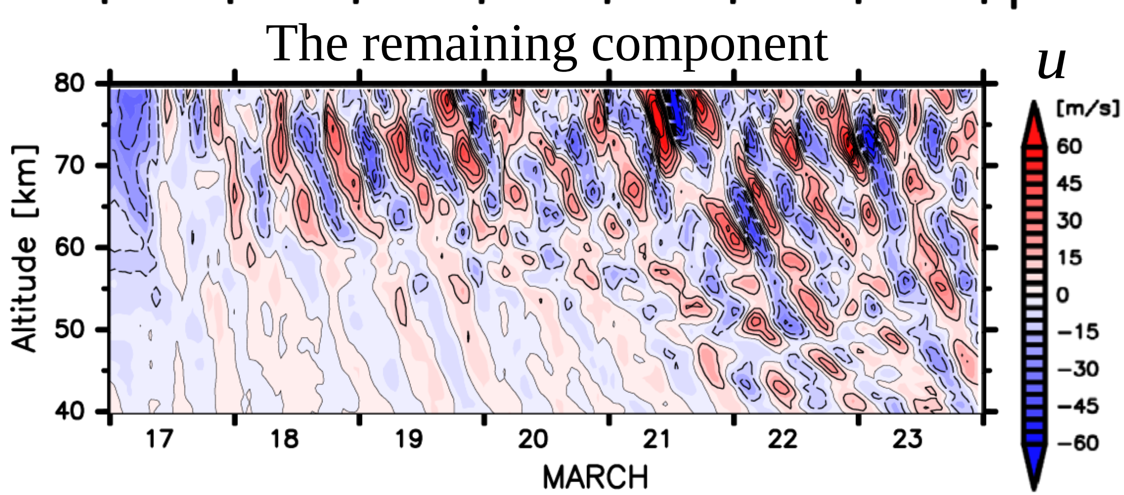

・The remaining component is similar to the simulated structure
— suggesting that the dominant wave structure is due to the remaining component

The remaining component

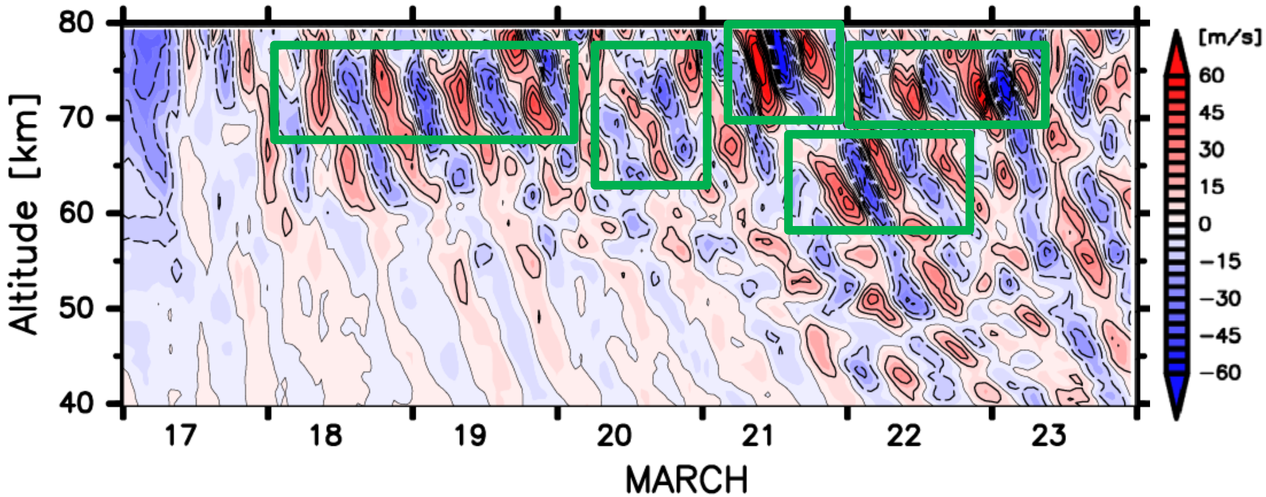

- Several wave packets cross over Syowa Station
  — This feature becomes clearer by using the Hilbert transform method (Sato et al., 2013)

The envelop function

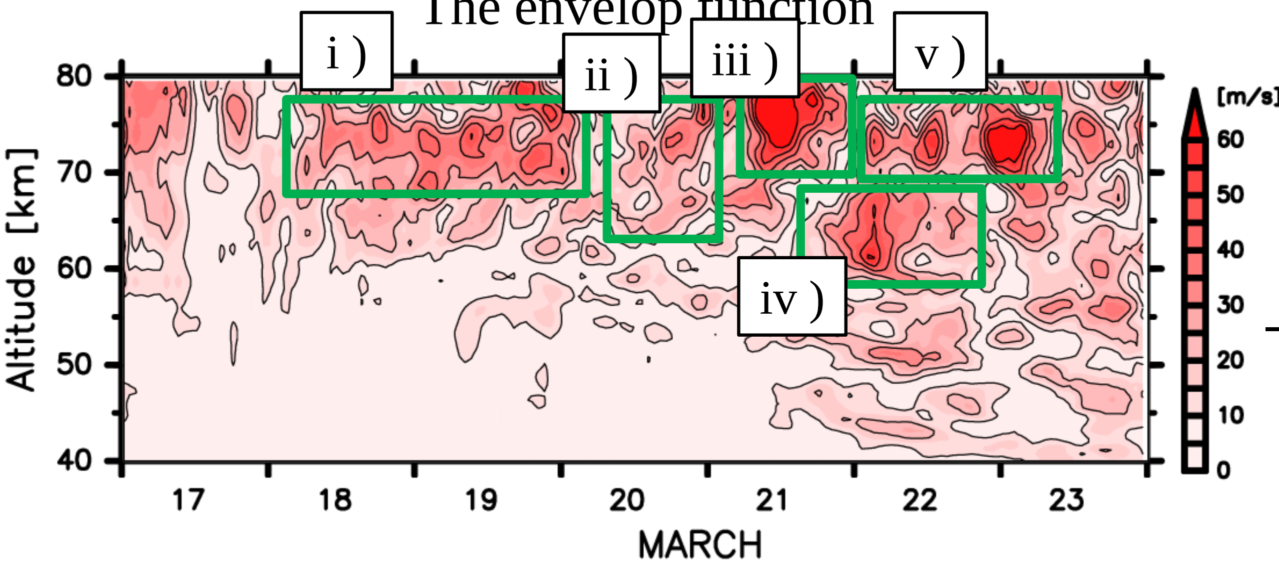

- We have labeled the dominant packets as (i) to (v)
  — Wave parameters of each packet are estimated
- m and ω are estimated using the above figure

- To obtain the horizontal structures of the wave packets, **composite maps of zonal wind components** have been made

— The grid point having local maxima of zonal wind components near Syowa Station is chosen as a reference point

— The average is taken for the period when the packet crosses over Syowa Station

- Results:

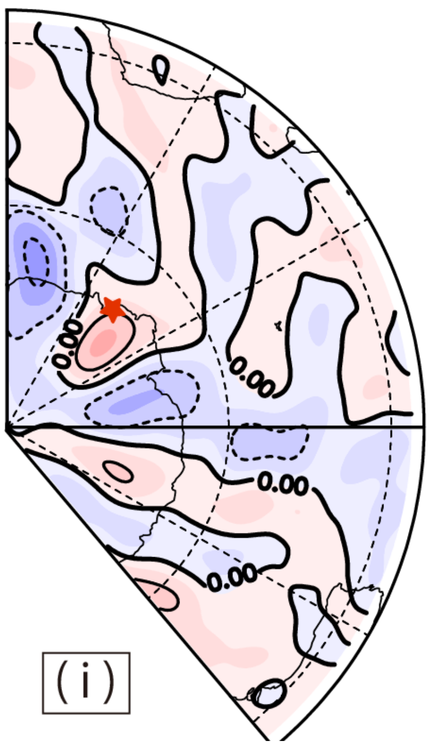

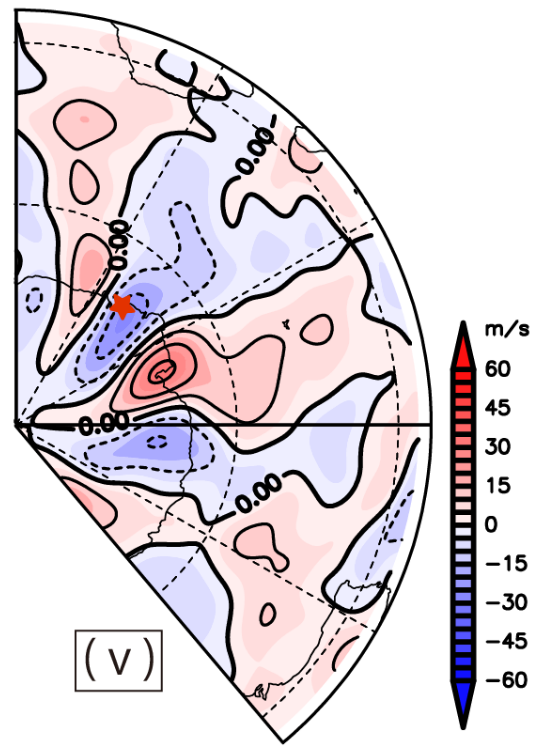

$\Rightarrow$ $2\pi/|k| \sim 2530$ km, $|l| \sim 0.0$ m^{-1}

$\Rightarrow$ $2\pi/|k| \sim 1660$ km, $2\pi/|l| \sim 7660$ km

■ Directly estimated wave parameters

Packet	k (m^{-1})	l (m^{-1})	m (m^{-1})	ω (s^{-1})	c_{p_x} (m s^{-1})	c_{p_z} (m s^{-1})	$\frac{f}{\hat{\omega}}$
(i) z = 70 km 3/18 12 UTC ~ 3/19 24 UTC	-2.48×10^{-6} (2530 km)	~ 0	**3.96×10^{-4} (15.8 km)**	**1.42×10^{-4} (12.3 h)**	−57.3	−0.36	0.763
(ii) z = 70 km 3/20 05 UTC ~ 3/21 01 UTC	-3.18×10^{-6} (1980 km)	-0.98×10^{-6} (6440 km)	**4.10×10^{-4} (15.3 km)**	**1.47×10^{-4} (11.8 h)**	−4.62	−0.36	0.704
(iii) z = 75 km 3/21 03UTC ~ 3/22 03 UTC	-2.79×10^{-6} (2250 km)	-2.48×10^{-6} (2530 km)	**3.92×10^{-4} (16.0 km)**	**1.99×10^{-4} (8.8 h)**	−71.3	−0.51	0.617
(iv) z = 65 km 3/21 21UTC ~ 3/22 09 UTC	-3.35×10^{-6} (1880 km)	-2.78×10^{-6} (2530 km)	**4.63×10^{-4} (13.6 km)**	**1.46×10^{-4} (11.9 h)**	−43.5	−0.32	0.617
(v) z = 72 km 3/22 02 UTC ~ 3/23 02 UTC	-3.78×10^{-6} (1660 km)	-0.82×10^{-6} (7660 km)	**4.52×10^{-4} (13.9 km)**	**1.59×10^{-4} (11.0 h)**	−42.1	−0.35	0.653
PANSY			**4.59×10^{-4} (13.7 km)**	**1.42×10^{-4} (12.3 h)**		**−0.30**	

- The estimated wave parameters in NICAM agree well with those by the PANSY radar
- These parameters are quite consistent with the linear theory of the hydrostatic inertia-gravity waves:

$$(\omega - kU)^2 = f^2 + \frac{N^2\left(k^2 + l^2\right)}{m^2}$$

The quasi 12-h disturbances are likely due to **large-scale inertia-gravity waves**

4. Numerical results: Propagation and generation mechanism

・We made an idealized backward ray tracing analysis of the inertia-gravity wave (e.g. Marks and Eckermann 1995)

— The estimated wave parameter is used in the ray tracing analysis

Packet (v)

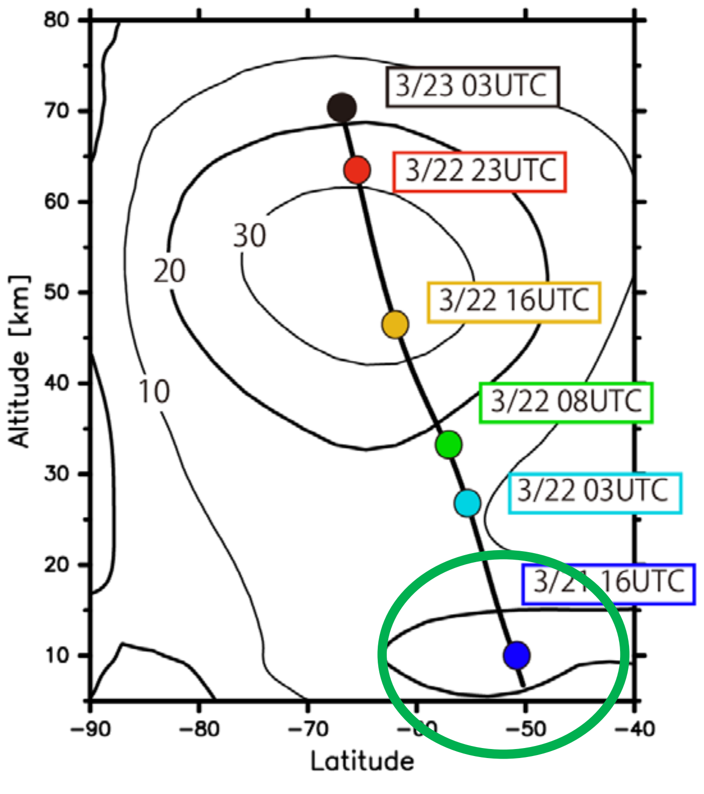

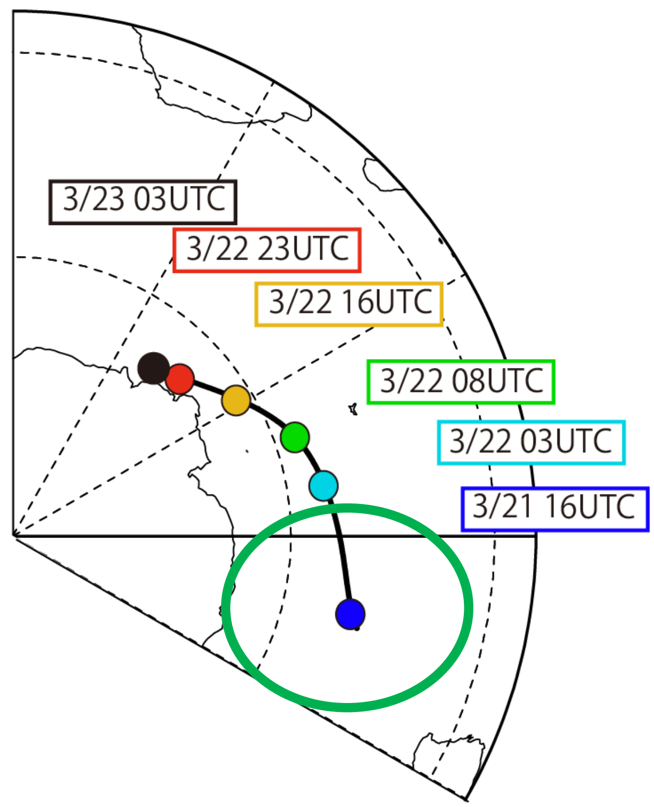

・The source of the inertia-gravity wave can be at any altitude along the ray above the lowest traceable altitude

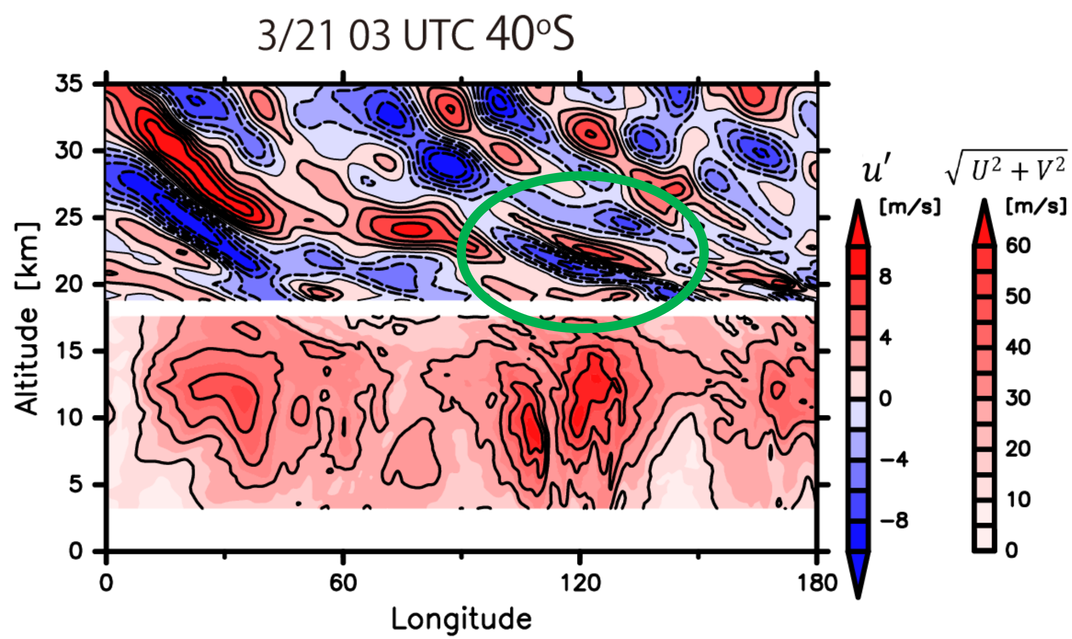

- It seems that the wave packet is **"captured"** around the tropospheric jet stream (Bühler & McIntyre 2005)

- The tropospheric jet stream strongly meandered and was imbalanced

z = 10 km

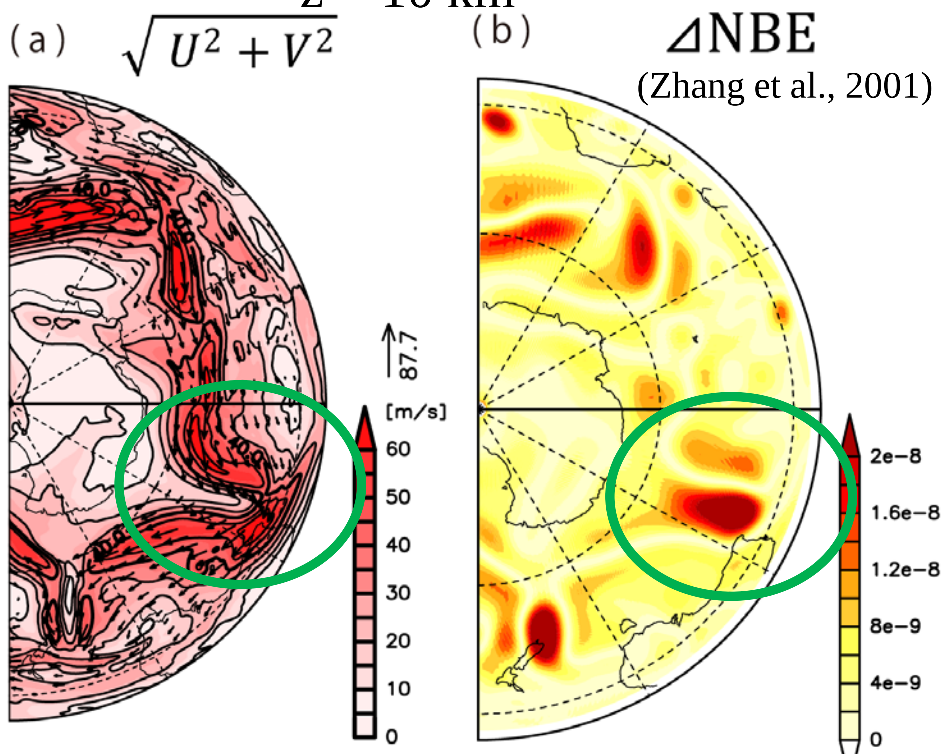

- The packet (v) was generated through **the spontaneous adjustment process** of the imbalanced tropospheric jet stream (Plougonven & Snyder, 2007)

5. Discussion

- Such a quasi-12 h disturbance in the polar region was also examined by many previous studies

  — most previous studies suggested that this disturbance is due to **tides:**

  Semi-diurnal migrating **tides**:
  — Fraser et al. (1990), Fisher et al. (2002)

  Semi-diurnal non-migrating **tides**:
  — Hernandez et al. (1993), Forbes et al. (1995), Fritts et al. (1998)
  Portnyagin et al. (1998), Yamashita et al. (2002), Wu et al. (2003)

  "**Pseudo-tide**" mechanism (GW momentum deposition induced by **tides**):
  — Waterscheid et al. (1986), Collins et al. (1992)

- This study first suggests that a quasi-12 h disturbance is due to large-scale inertia-gravity waves, which are generated through the spontaneous adjustment process of the tropospheric jet stream

6. Conclusion

- Large-amplitude disturbances with a period of about 12 h in the mesosphere were examined by using the PANSY radar and the numerical simulation with NICAM

The disturbances were **due to the large-scale inertia-gravity waves** with horizontal wavelength more than 1500 km, **not due to the semi-diurnal tides**

— the wave parameters estimated using NICAM agree quite well with those estimated using the PANSY radar observation

The wave packets simulated over Syowa Station were likely generated through **the spontaneous adjustment** of the tropospheric jet stream and the polar night jet (not shown)

- Statistical studies are needed to examine the seasonality of the large-scale inertia-gravity waves by using the observational data and the numerical simulations

4. Numerical results: the MERRA reanalysis dataset

Since the horizontal scale of the quasi-12 h disturbance is large (> 1000 km),
the disturbances may be also resolved in the MERRA reanalysis dataset

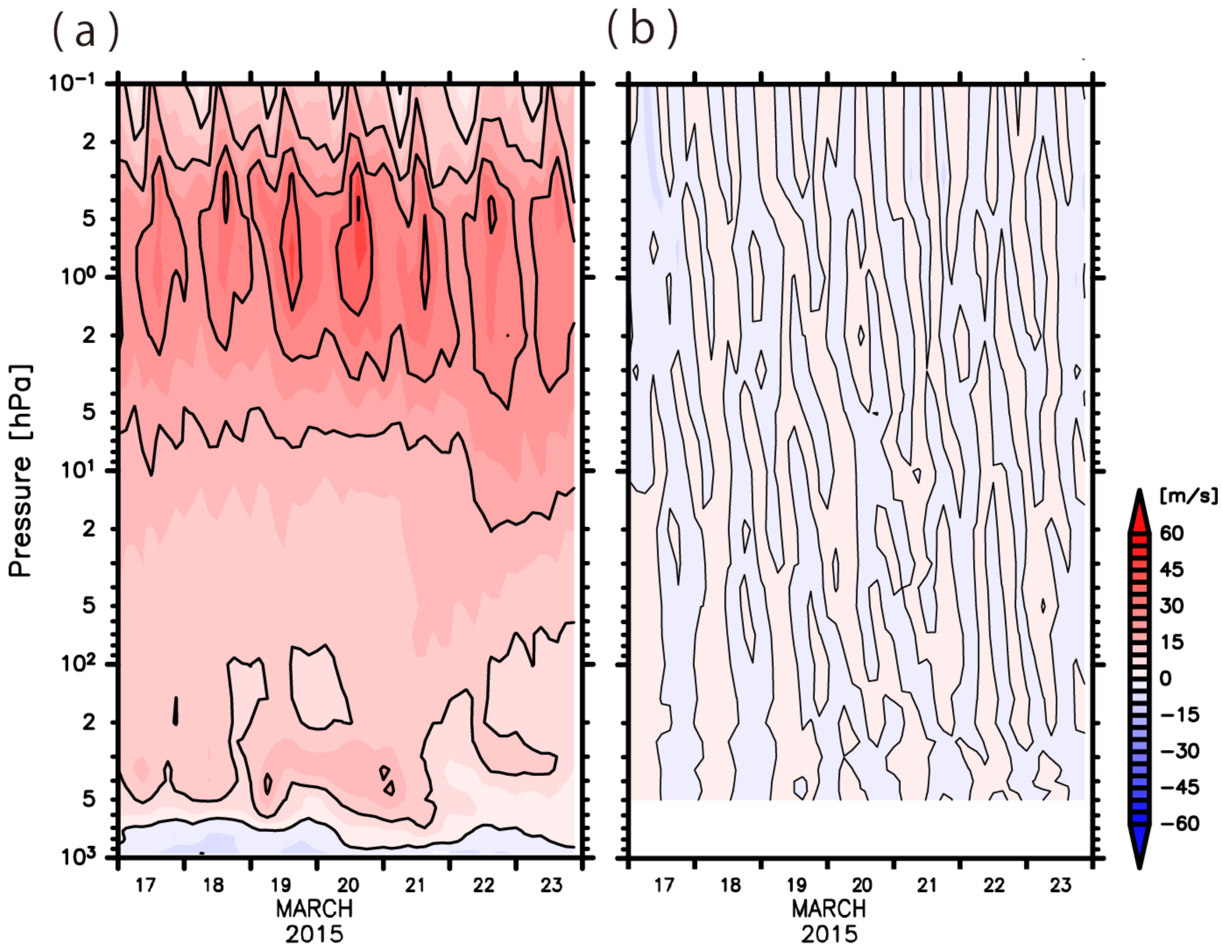

The MERRA reanalysis dataset does not fully resolved the quasi 12-h oscillation
— likely due to their coarse vertical resolution (5 grid points in the range of 16 km)

1. Introduction

G – Gravity waves
P – Planetary waves
S – Synoptic scale waves

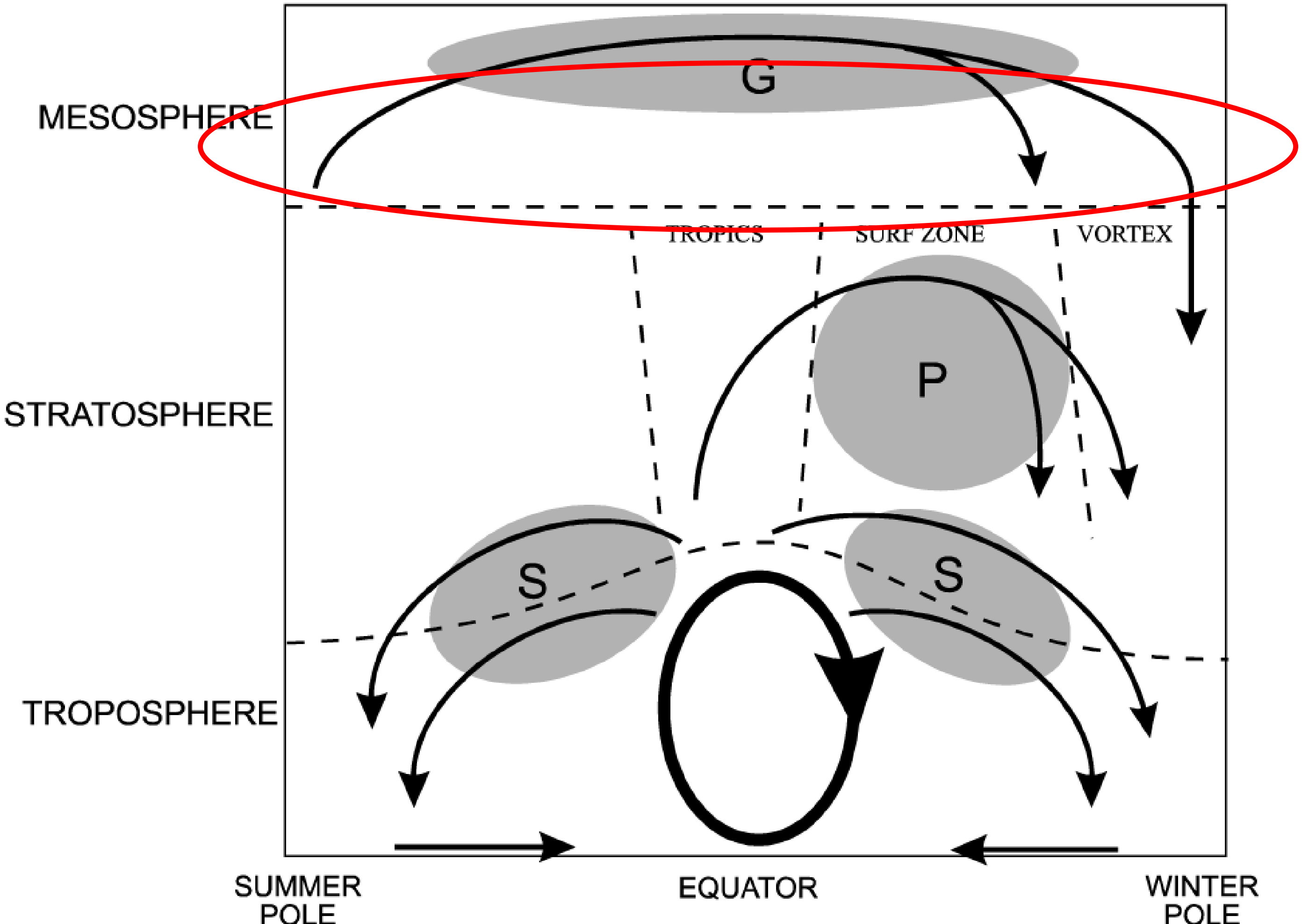

Plumb (2002)

- Propagation paths and breaking regions of gravity waves are not globally uniform

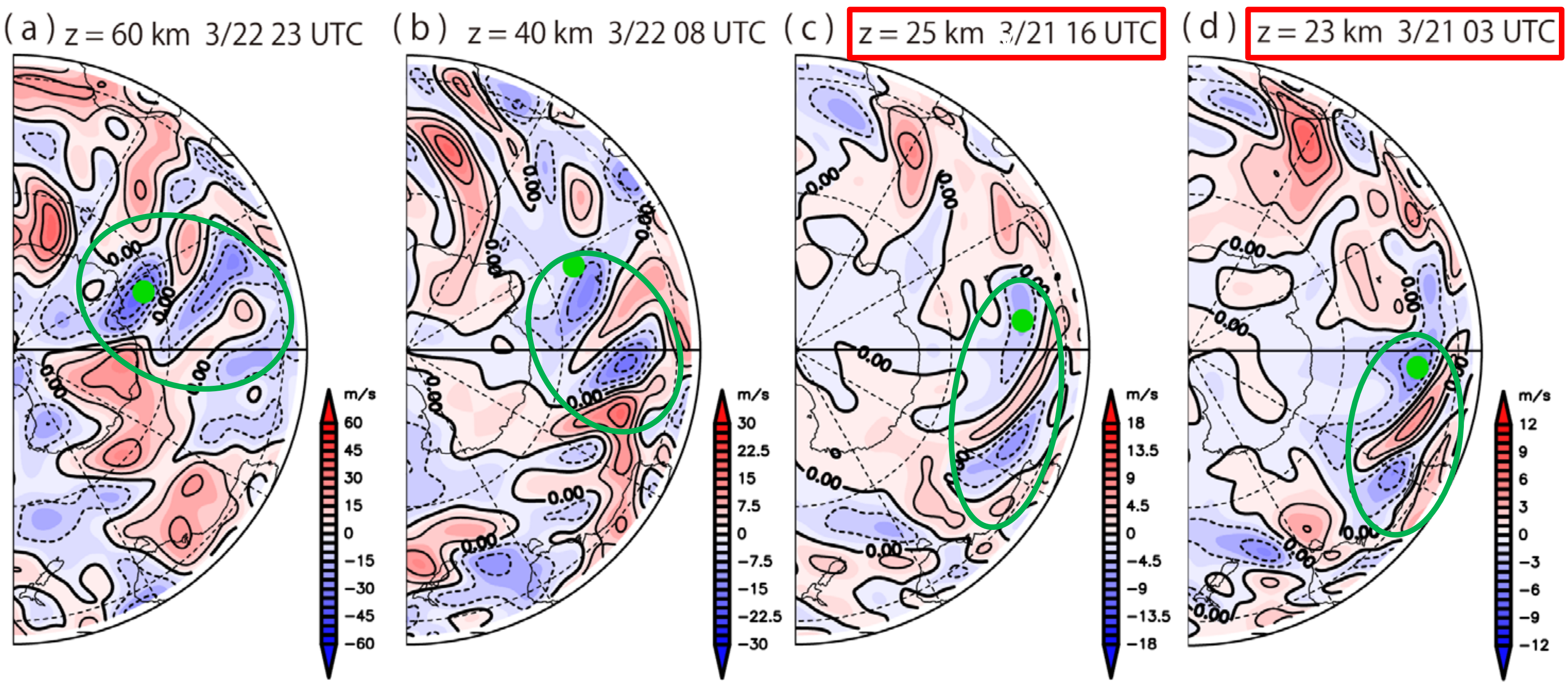

- The wave packet propagate from around (100°E, 40°S) to Syowa Station
  — The propagation path detected by this method agrees well with the path detected by the classical ray tracing method

- In the lower stratosphere, the propagation of the wave packet is very slow compared with that located in the upper stratosphere

4. Numerical results: Propagation and generation mechanism

Packet (v)

02 UTC 23 March, z = 70 km

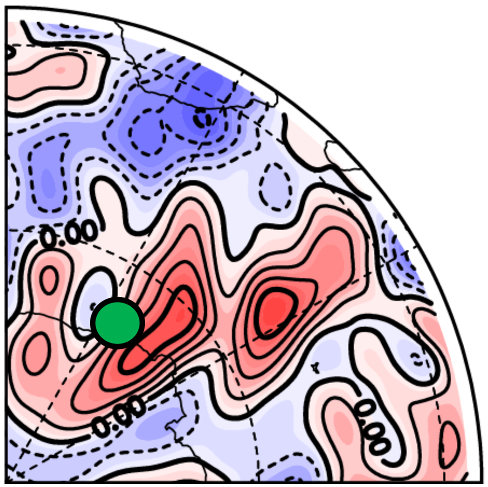

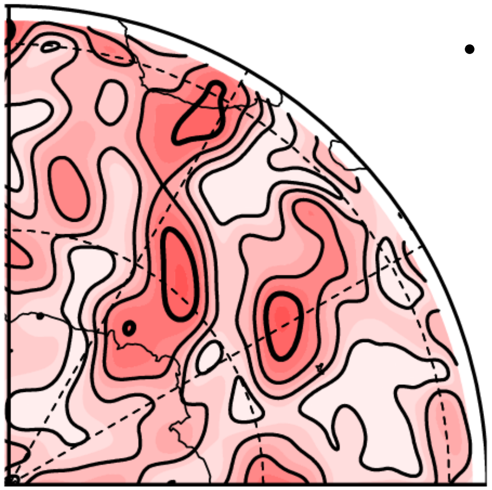

- The location of the packet at an altitude is determined by the local maxima of the envelop function

— By tracing the location of the packet backward and downward, the propagation path of the packet can be examined

69°S, z = 70 km

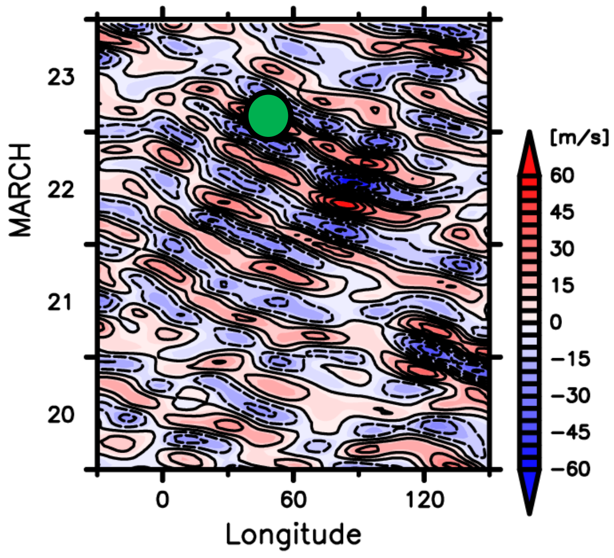

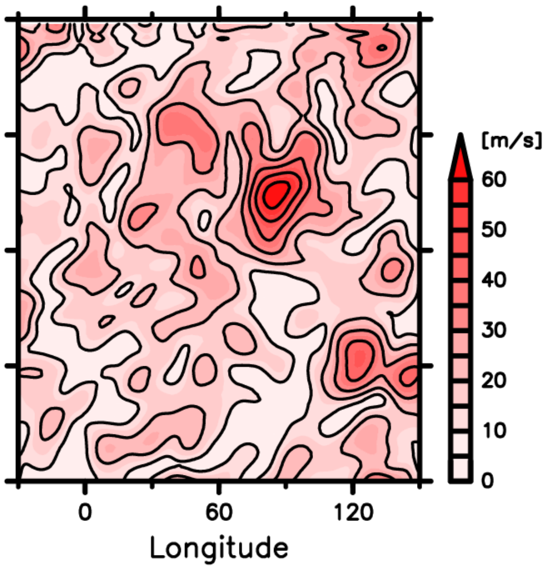

4. Numerical results: Propagation and generation mechanism

- A wave packet is likely generated through the spontaneous adjustment process of the polar night jet

$\sqrt{\rho_0}u'$

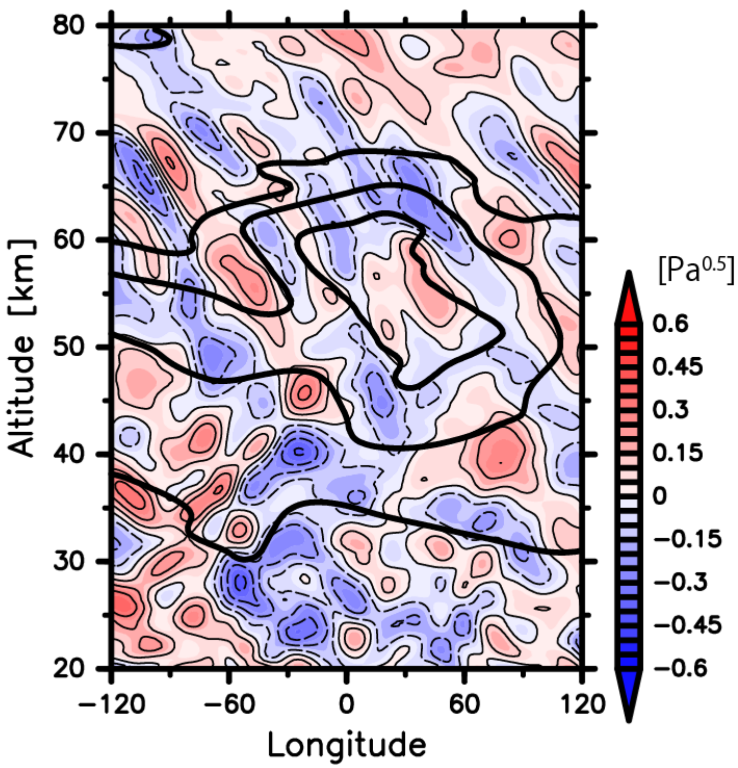

$\overline{p'w'}$

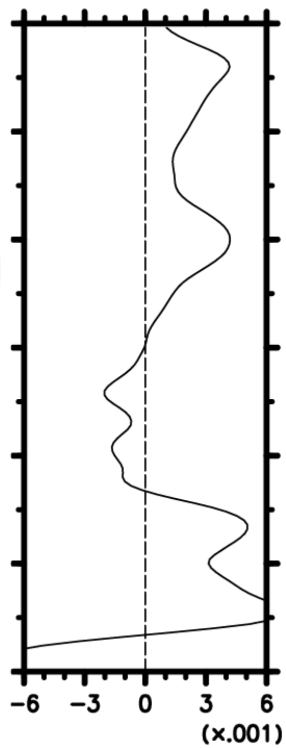

An idealized experiment
(Yasuda et al., 2015)

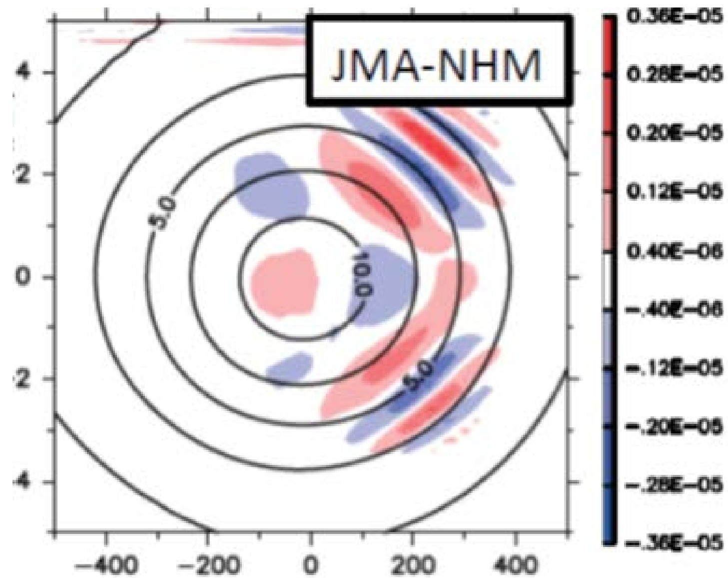

4. Numerical results: Propagation and generation mechanism

- The polar night jet is not imbalanced and does not strongly meander

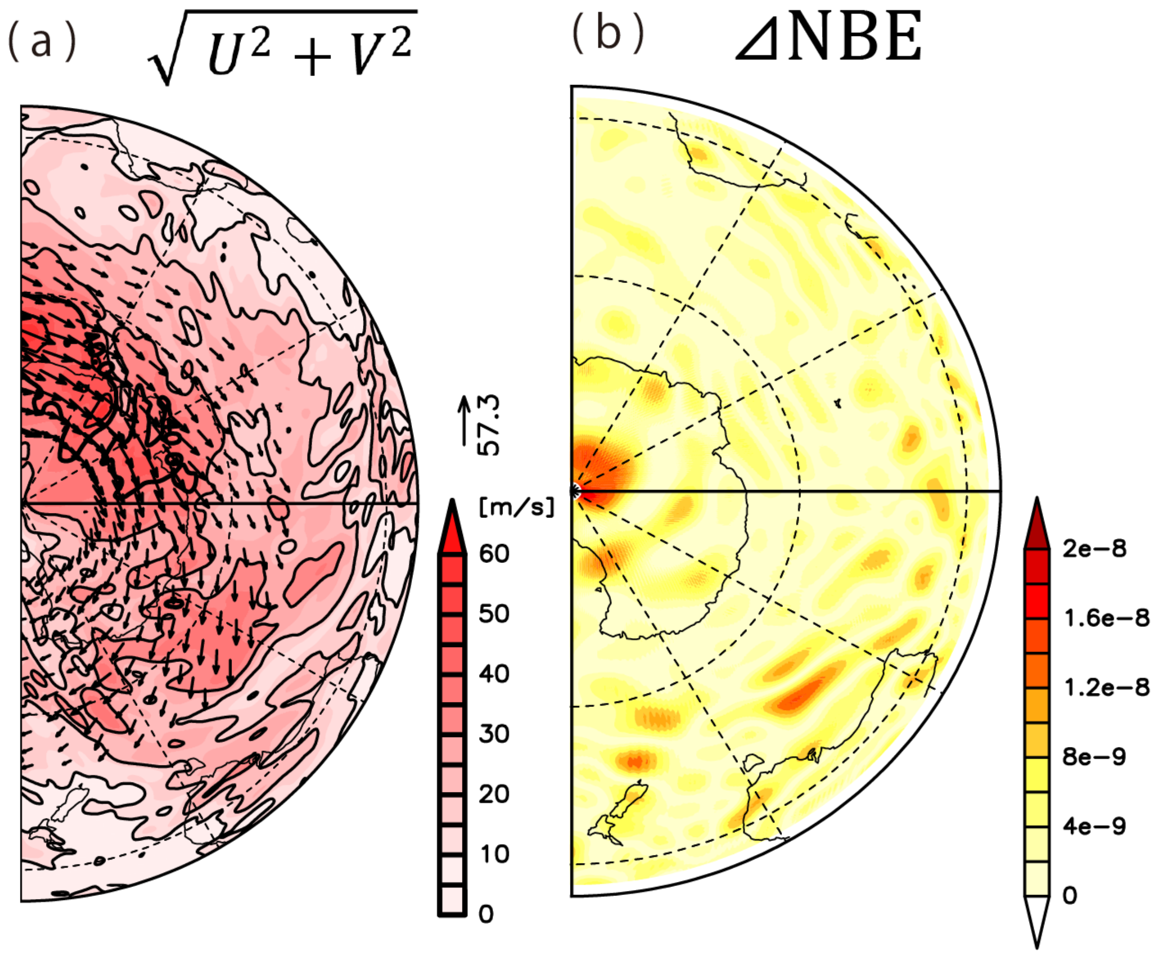

4. Numerical results: the momentum fluxes and energies

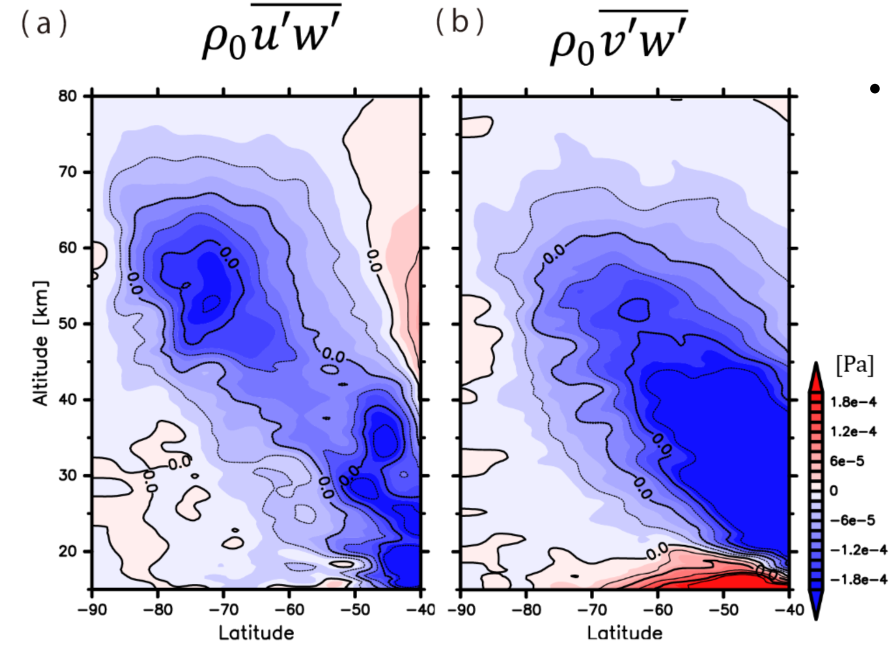

- The zonal and meridional momentum fluxes exhibit a slanted structure from the lower-stratosphere to the mesosphere

  — suggesting the waves focusing into the polar vortex (Sato et al. 2009)

- According to the linear theory of the inertia-gravity waves, by using the vertical kinetic energy $\overline{VE}$ and the potential energy $\overline{PE}$, we can derive

$$\frac{f}{\hat{\omega}} = \frac{f}{N}\sqrt{\frac{\overline{VE}}{\overline{PE}}}$$

where

$$\overline{VE} = \frac{1}{2}\rho_0 \overline{w'^2}, \quad \overline{PE} = \frac{1}{2}\rho_0 \overline{\frac{g^2}{N^2}\left(\frac{T'}{T}\right)^2}$$

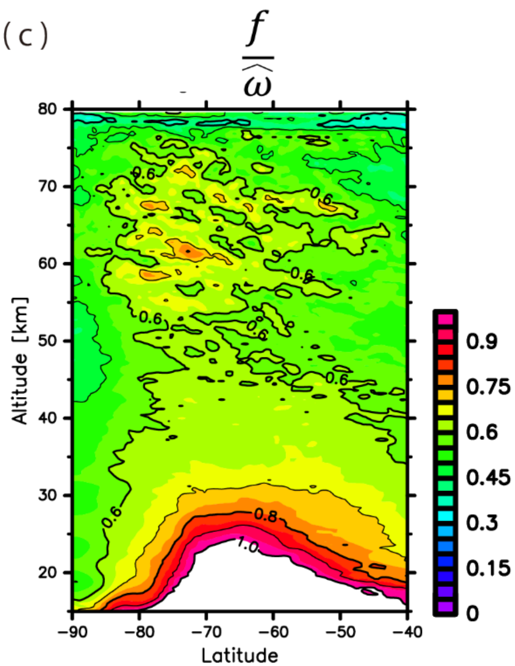

Packet	$\frac{f}{\hat{\omega}}$
(i)	0.763
(ii)	0.704
(iii)	0.617
(iv)	0.617
(v)	0.653

- The estimated intrinsic frequencies are quite consistent with each other